Southern Hemisphere Summer Mesopause Responses to El Niño–Southern Oscillation

TAO LI,[a,b] NATALIA CALVO,[c] JIA YUE,[d] JAMES M. RUSSELL III,[d] ANNE K. SMITH,[e] MARTIN G. MLYNCZAK,[f] AMAL CHANDRAN,[g] XIANKANG DOU,[a,b] AND ALAN Z. LIU[h]

[a] *CAS Key Laboratory of Geospace Environment, School of Earth and Space Sciences, University of Science and Technology of China, Hefei, Anhui, China*
[b] *Mengcheng National Geophysical Observatory, School of Earth and Space Sciences, University of Science and Technology of China, Hefei, Anhui, China*
[c] *Departamento de Fisica de la Tierra II, Universidad Complutense de Madrid, Madrid, Spain*
[d] *Center for Atmospheric Sciences, Hampton University, Hampton, Virginia*
[e] *Atmospheric Chemistry Observations and Modeling Laboratory, National Center for Atmospheric Research,*[i] *Boulder, Colorado*
[f] *NASA Langley Research Center, Hampton, Virginia*
[g] *Laboratory for Atmospheric and Space Physics, University of Colorado Boulder, Boulder, Colorado*
[h] *Physical Science Department, Embry-Riddle Aeronautical University, Daytona Beach, Florida*

(Manuscript received 12 November 2015, in final form 30 May 2016)

ABSTRACT

In the Southern Hemisphere (SH) polar region, satellite observations reveal a significant upper-mesosphere cooling and a lower-thermosphere warming during warm ENSO events in December. An opposite pattern is observed in the tropical mesopause region. The observed upper-mesosphere cooling agrees with a climate model simulation. Analysis of the simulation suggests that enhanced planetary wave (PW) dissipation in the Northern Hemisphere (NH) high-latitude stratosphere during El Niño strengthens the Brewer–Dobson circulation and cools the equatorial stratosphere. This increases the magnitude of the SH stratosphere meridional temperature gradient and thus causes the anomalous stratospheric easterly zonal wind and early breakdown of the SH stratospheric polar vortex. The resulting perturbation to gravity wave (GW) filtering causes anomalous SH mesospheric eastward GW forcing and polar upwelling and cooling. In addition, constructive inference of ENSO and quasi-biennial oscillation (QBO) could lead to stronger stratospheric easterly zonal wind anomalies at the SH high latitudes in November and December and early breakdown of the SH stratospheric polar vortex during warm ENSO events in the easterly QBO phase (defined by the equatorial zonal wind at ~25 hPa). This would in turn cause much more SH mesospheric eastward GW forcing and much colder polar temperatures, and hence it would induce an early onset time of SH summer polar mesospheric clouds (PMCs). The opposite mechanism occurs during cold ENSO events in the westerly QBO phase. This implies that ENSO together with QBO could significantly modulate the breakdown time of SH stratospheric polar vortex and the onset time of SH PMC.

1. Introduction

As a result of sea surface temperature variation in the tropical east-central Pacific Ocean, El Niño–Southern Oscillation (ENSO) strongly impacts interannual variability not only in the tropical troposphere (Yulaeva and Wallace 1994) but also in the global middle atmosphere (e.g., the stratosphere and mesosphere; Randel et al. 2009; Calvo et al. 2010; Li et al. 2008, 2013; Pedatella and Liu 2013). Previous observations and model simulations have suggested

Denotes Open Access content.

[i] The National Center for Atmospheric Research is sponsored by the National Science Foundation.

Corresponding author address: Tao Li, School of Earth and Space Sciences, University of Science and Technology of China, 96 Jinzhai Rd., Hefei, Anhui 230026, China.
E-mail: litao@ustc.edu.cn

DOI: 10.1175/JCLI-D-15-0816.1

significant middle atmosphere temperature anomalies during El Niño, with an equatorial stratosphere cooling and a Northern Hemisphere (NH) high-latitude warming (Garcia-Herrera et al. 2006). This is induced by the anomalously increased planetary wave (PW) propagation (from the troposphere) and PW dissipation in the stratosphere of NH high latitudes, leading to anomalous wave dissipation, decelerated stratospheric westerly zonal wind, and an enhanced Brewer–Dobson circulation (Sassi et al. 2004; Manzini et al. 2006; Hardiman et al. 2007; Calvo et al. 2010).

By analyzing temperature profiles observed by the Sounding of the Atmosphere Using Broadband Emission Radiometry (SABER) instrument, Li et al. (2013) found a tropical warming and NH high-latitude cooling in the mesosphere, opposite to its stratospheric pattern, during warm ENSO events in NH winter. However, the anomalous temperature induced by ENSO in the summer polar mesopause of the Southern Hemisphere (SH) has not yet been investigated in the observations, and the details of the coupling mechanism have not yet been explored with an advanced climate model. The summer polar mesopause temperature anomalies can influence the variability of polar mesospheric clouds (PMCs), usually located at ~80–85-km height. Recent satellite observations already found dramatic interannual variability of the PMC onset time (Karlsson et al. 2011) and occurrence frequency (Gumbel and Karlsson 2011).

In this paper, we target these key unknowns using observations by SABER, onboard the *Thermosphere–Ionosphere–Mesosphere Energetics and Dynamics* (*TIMED*) satellite, and by the Microwave Limb Sounder (MLS), onboard the *Aura* satellite, together with the Whole Atmosphere Community Climate Model (WACCM) simulations and the European Centre for Medium-Range Weather Forecasts (ECMWF) interim reanalysis dataset. Our goal is to show monthly mean temperature response to ENSO in the SH summer mesopause region and the possible influence of ENSO on the onset time of SH PMCs. For the latter, we use PMC measurements made by the solar backscatter ultraviolet (SBUV) instruments in Benze et al. (2012). Both Karlsson et al. (2011) and Benze et al. (2012) found that the PMC onset time is well correlated with the timing of breakdown of SH stratospheric polar vortex. This SH stratospheric polar vortex influences the propagation of gravity waves (GWs) into the mesopause region and thus the mesopause temperature. As such, the stratospheric control to mesopause temperature mainly induces the variation of PMC onset (Karlsson et al. 2011). Hervig et al. (2009) also concluded that the PMC seasonal dependence is generally controlled by temperature. Rong et al. (2014) found that during the summer season start and end, the temperature plays a dominant role in influencing the PMC variability.

Therefore, we focused our study here only on the impact of the polar mesopause temperature on the PMC onset time. First, we describe the datasets and analysis method in section 2 and then present the observational and model results of summer polar mesopause temperature and ozone response to ENSO in section 3. In section 4, we examine the SH stratosphere anomalies during the ENSO events and propose a coupling mechanism to explain the observed anomalies. In section 5, we discuss how ENSO together with the quasi-biennial oscillation (QBO) could impact the onset time of SH summer polar PMCs. A summary is then presented in section 6.

2. Datasets and analysis

The *TIMED*/SABER observations and WACCM model have been discussed in detail by Li et al. (2013). In short, SABER temperature profiles are retrieved from CO_2 atmospheric limb emission profiles in the 15-μm band (Russell et al. 1999). We use the version 2.0 SABER data, which are available between January 2002 and February 2016 (available at http://saber.gats-inc.com/). First, we calculate the daily mean temperatures separately for ascending and descending phases in 5° latitude bins, respectively, at 80°S, 75°S, . . . , up to 50°N. At every latitude, the daily mean profiles are then averaged within a ~60-day window centered in April, August, and December between 80° and 55°S (only these periods include data at high SH latitudes) and centered at every month between 50°S and 50°N (available for all months). Since it takes ~60 days for SABER to complete a nearly 24-h local time sampling, we use the SABER data centered in December, covering data from the middle of November to the middle of January, to reduce tidal aliasing.

The *Aura* MLS has been retrieving middle atmosphere temperature profiles from limb emission measurements in the microwave since August 2004. Temperature profiles between 261 and 0.001 hPa (~92 km) are retrieved from 118- and 240-GHz radiances of O_2 spectra (Schwartz et al. 2008). The *Aura* satellite is in a near-polar (82°S–82°N) sun-synchronous orbit with ascending footprints crossing the equator at ~1400 LT and descending at ~0200 LT. Here we use MLS, version 4.2, temperature profiles from August 2004 to February 2016 (available at http://disc.sci.gsfc.nasa.gov/Aura/data-holdings/MLS/index.shtml). Similar to SABER, we calculate the daily zonal mean temperatures separately for ascending and descending phases within 5° latitude bins centered at 80°S, 75°S, . . . , up to 80°N, and then at each latitude we form monthly mean profiles by averaging all daily mean profiles in each month.

We use a four-member ensemble of WACCM version 3.5 simulations between 1953 and 2005 (Calvo et al.

TABLE 1. Date and corresponding maximum values of N3.4 index for strong warm and cold ENSO events.

Warm event	N3.4 index	Cold event	N3.4 index
January 1958	1.52	November 1955	−2.26
November 1965	1.31	November 1964	−1.34
December 1972	1.83	January 1971	−1.75
December 1982	2.14	December 1971	−1.21
January 1992	1.69	November 1973	−2.26
December 1994	1.22	January 1976	−1.93
November 1997	2.33	December 1984	−1.27
November 2002	1.37	November 1988	−1.93
December 2006	1.09	January 1999	−1.58
December 2009	1.43	January 2000	−1.71
November 2015	2.37	January 2008	−1.50
		January 2011	−1.47

2010), with a 1.9° × 2.5° (latitude × longitude) horizontal resolution to compare with satellite observations. These model runs use prescribed sea surface temperature based on observations; therefore, the date of the ENSO events and their magnitude in SST anomalies in the model is based on observations. The QBO was not self-generated in the WACCM but imposed by nudging to the observed equatorial zonal wind in the lower stratosphere. Therefore, we also use the ECMWF interim reanalysis dataset (Dee et al. 2011) between 1979 and 2014 (available at http://apps.ecmwf.int/datasets/data/interim-full-moda/) to reveal the QBO effects in the stratosphere.

We then apply a multivariate linear regression analysis to the deseasonalized monthly (WACCM, ECMWF, and MLS) or bimonthly (SABER) mean profiles. The detailed analysis method can be found in Li et al. (2013). The regression analysis fits the linear trend, the 11-yr solar cycle, quasi-biennial oscillation (QBO), and the stratospheric volcanic aerosols. The residuals then include any ENSO signal. The ENSO events are determined to occur when the monthly mean Niño-3.4 index (N3.4) is greater than 1 (~1.2 standard deviation) between 1953 and 2014. The N3.4 index is the observed sea surface temperature anomaly averaged over 120°–170°W and 5°S–5°N (available at http://www.cpc.ncep.noaa.gov/data/indices/ersst4.nino.mth.81-10.ascii). Table 1 lists the dates of warm and cold ENSO events since 1953 with all events maximized in the late fall and winter. Composite differences in December during ENSO events are calculated by subtracting the residual during cold ENSO events from that during warm events (warm minus cold events). The 95% significance regions are estimated with a Monte Carlo method, similar to that used by Calvo et al. (2010). For easy comparison between the WACCM model and the satellite observations, the composite anomaly is then formed by directly dividing the composite difference of the residual by the composite difference of the N3.4 index. The N3.4 composite difference between warm and cold ENSO events in December is ~3.2 for the 1953–2005 period (WACCM) and the 1979–2015 period (ECMWF) and ~2.8 for the 2002–15 period (satellites). To extract the anomaly only related to the QBO from the ECMWF dataset, we fit the deseasonalized time series with a linear trend, solar cycle, ENSO, and volcanic aerosol and leave out QBO oscillation in the residuals. The composite difference due to the QBO (easterly minus westerly phase) is then formed.

3. Results

The climatological zonal mean temperature in December is characterized by a cold SH summer mesopause (<150 K) and a warm NH winter mesopause (>200 K) due to a summer pole to winter pole circulation driven by the eastward GW drag in SH summer mesopause and westward GW drag in NH winter mesopause. We show in Fig. 1 the composite anomalies of zonal mean temperature observed by SABER (left) and MLS (center) and simulated by WACCM (right) in the mesosphere and lower-thermosphere region in December. It is evident that these three datasets reveal similar latitude–altitude patterns in temperature anomalies. In the SH polar region, the satellite observations reveal a significant cooling of 2.5–3.5 K $(\mathrm{N3.4})^{-1}$ in the upper mesosphere (70–95 km) and a significant warming of ~8 K $(\mathrm{N3.4})^{-1}$ in the lower thermosphere during warm ENSO events. A midmesosphere warming and a mesopause cooling are also observed in the equatorial region. The morphology of the observations is consistent with the simulations, but the observed magnitude of the changes is ~3–5 times stronger than simulations. Li et al. (2013) focused on the ENSO midmesospheric temperature anomalies in the tropics and NH, which are due to the anomalous residual meridional circulation driven by the anomalous GW wave forcing. The present analysis extends to the lower thermosphere (up to 110 km) and focuses on the Southern Hemisphere polar region, beyond the range investigated by Li et al. (2013).

We show in Fig. 2 the composite anomalies of GW forcing (left) and residual meridional circulation (right) in the MLT region derived from WACCM3.5. The simulations show a strong upper mesosphere eastward GW forcing anomaly at the SH high latitudes, with a maximum of ~3 m s^{-1} day^{-1} $(\mathrm{N3.4})^{-1}$ during warm ENSO events. This eastward GW forcing anomaly corresponds to a strong anomalous upwelling residual circulation and cooling (Fig. 1) in the upper mesosphere of the SH polar region. We note here that anomalous GW forcing is the primary contributor to the anomalous total wave forcing in the mesosphere. In the lower thermosphere of SH

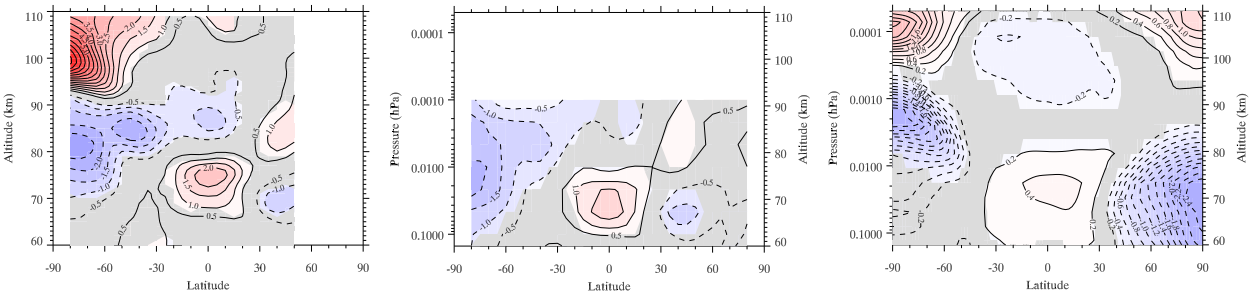

FIG. 1. The ENSO composite anomalies (warm minus cold events) of zonal mean temperature observed by (left) SABER and (center) MLS and simulated by (right) WACCM in the mesopause region in December. The contour interval is 0.5 K $(N3.4)^{-1}$ for satellite observations and 0.2 K $(N3.4)^{-1}$ for WACCM. Red represents positive response and blue represents negative; the gray regions denote confidence levels below 95% (1.96σ).

high latitudes, downwelling and an opposite but weak GW forcing anomaly can clearly be seen with a maximum rate of $\sim -1\,\mathrm{m\,s^{-1}\,day^{-1}}\,(N3.4)^{-1}$. Although the anomalous downwelling in the NH polar lower thermosphere is stronger than that in the SH, the magnitude of the simulated anomalous warming in the NH pole is weaker than that in the SH (Fig. 1c). This is possibly due to more solar absorption by tracer gases during SH polar day than during the NH polar night and/or to differences in the eddy diffusion caused by GWs. We also note that the residual meridional circulation anomaly in the lower thermosphere region is clearly opposite to the mesosphere anomaly, consistent with the temperature anomalies shown in Fig. 1.

4. Coupling mechanism

Since the anomalous eastward GW forcing in the upper mesosphere of the SH high latitudes is likely induced by the anomalous zonal wind filtering below the mesosphere, we show in Fig. 3 the WACCM composite anomalies of stratospheric temperature (left), zonal wind (center), and Eliassen–Palm (EP) flux divergence (right). The equatorial stratospheric cooling (whole stratosphere range) and NH high-latitude warming during warm ENSO events (Fig. 3, left), indicated by SABER observations (Li et al. 2013), are induced by the enhanced Brewer–Dobson circulation as a result of enhanced PW propagation and dissipation (Fig. 3, right) at the NH high latitudes (Sassi et al. 2004). The anomalous easterly zonal wind in the SH high-latitude stratosphere (Fig. 3, center) suggests the modulation of ENSO on the SH stratosphere polar vortex. The SH polar stratospheric warming below 10 hPa (~30 km) is likely a sign of early SH polar vortex breakdown during warm ENSO events. It is also clear that the anomalous stratospheric easterly zonal wind at the NH high latitudes, driven by the anomalous westward EP flux divergence during the warm ENSO events (Fig. 3, right), is much stronger than that in the SH. However, there is no clear anomalous EP flux divergence in the SH stratosphere, suggesting that the anomalous SH stratospheric easterly zonal wind is most likely a manifestation of

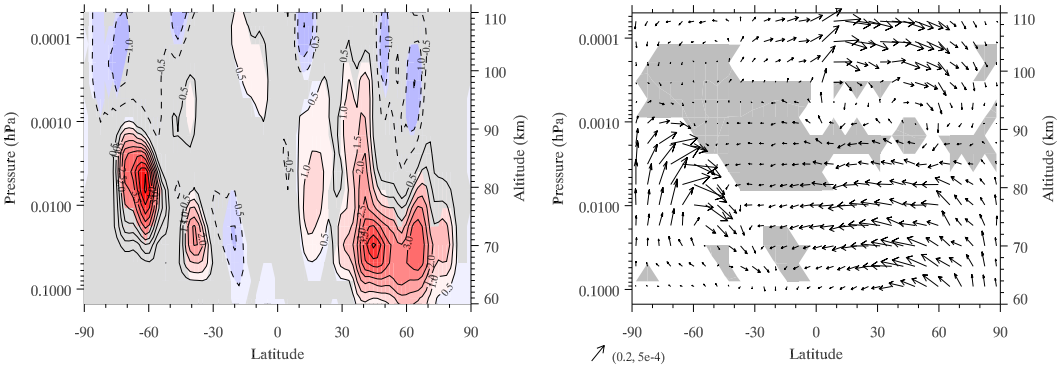

FIG. 2. As in Fig. 1, but for WACCM (left) GW forcing and (right) residual meridional circulation ($\overline{v}^*$, $\overline{w}^*$), where $\overline{v}^*$ and $\overline{w}^*$ are the transformed Eulerian mean meridional and vertical velocities (Andrews and McIntyre 1976). The contour line interval is 0.5 m s^{-1} day^{-1} $(N3.4)^{-1}$. The maximum values of $\overline{v}^*$ and $\overline{w}^*$ [m s^{-1} $(N3.4)^{-1}$] are shown at the bottom-left corner of the right panel.

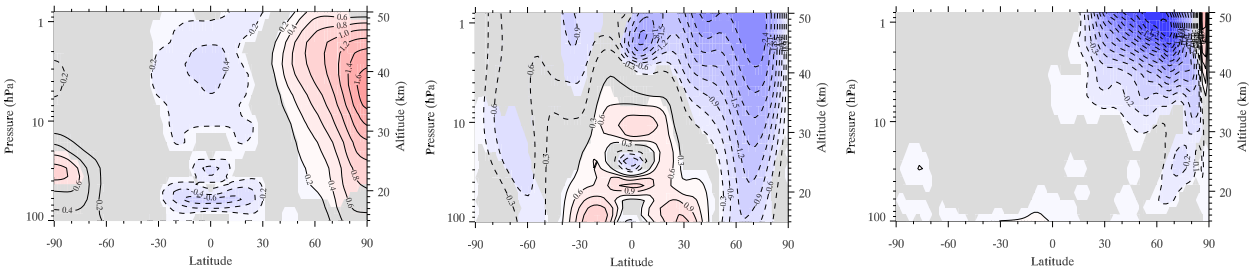

FIG. 3. As in Fig. 1, but for WACCM (left) stratospheric temperature, (center) zonal wind, and (right) EP flux divergence. The contour line interval is 0.2 K $(N3.4)^{-1}$ for temperature, 0.3 m s^{-1} $(N3.4)^{-1}$ for zonal wind, and 0.1 m s^{-1} day^{-1} $(N3.4)^{-1}$ for EP flux divergence.

anomalous easterly zonal wind shear induced by the anomalous meridional temperature gradient between the SH polar region and the equator. The anomalous meridional temperature gradient in the SH lower stratosphere is roughly ~0.015 K (degree latitude)$^{-1}$ (with ~0.8 K at the SH pole and ~−0.6 K at the equator, shown in the left panel of Fig. 3), and the estimated anomalous meridional wind difference between 20 and 100 hPa at 60°S is ~−0.5 m s^{-1} according to the thermal wind equation. This is consistent with the results shown in the center panel of Fig. 3.

The climatological zonal mean zonal wind at the SH high latitudes in December is characterized by a weak westerly in the lower stratosphere and an increased easterly with altitude in the upper stratosphere and lower mesosphere. During warm ENSO events in December, less eastward- and upward-propagating GWs are filtered by the weakened lower-stratosphere westerly (eastward) zonal wind at the SH high latitudes, while more westward-propagating GWs are filtered by the strengthened upper-stratosphere easterly (westward) zonal wind. The net effect is that the eastward GW forcing in the SH mesosphere is thus enhanced (anomalous eastward forcing shown in the left panel of Fig. 2), strengthening the SH mesospheric residual meridional circulation with an anomalous SH polar mesosphere upwelling (Fig. 2, right). This part of the mechanism is similar to that proposed by Karlsson et al. (2011), who suggested that the SH polar mesopause temperature is impacted by the breakdown time of SH stratospheric polar vortex. The anomalous mesospheric westerly (eastward) zonal wind further induces the anomalous westward GW filtering in the lower thermosphere of SH high latitudes, leading to opposite residual meridional circulation to its mesospheric counterpart and downwelling in the polar region. The schematic diagram for the coupling mechanism is shown in Fig. 4.

During winters with strong PW activity in the NH stratosphere such as during El Niño, the NH polar stratosphere warms and the equatorial stratosphere cools; the opposite pattern is seen in the NH mesosphere. This pattern has been well established in observations and GCMs. The proposed interhemispheric coupling (IHC) mechanism that links the summer mesopause variability with that in the winter stratosphere (in January) is discussed by Becker et al. (2004), Karlsson et al. (2009), Körnich and Becker (2010), Siskind et al. (2011), Espy et al. (2011), and Murphy et al. (2012). According to this mechanism, warming and decreased westerly zonal wind in the NH high-latitude stratosphere caused by enhanced PW dissipation lead to weaker net westward GW forcing in the NH mesosphere. This then weakens the NH mesosphere residual meridional circulation and thus cools the NH polar mesosphere and warms the tropics. The tropical mesospheric warming increases the SH summer mesosphere meridional temperature gradient and therefore accelerates the SH easterly mesospheric zonal wind.

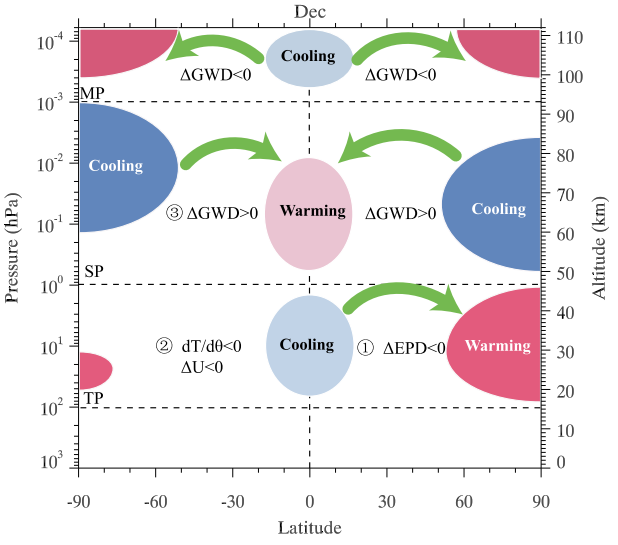

FIG. 4. The schematic diagram of the coupling mechanism during the warm ENSO events in December. Red represents warming and blue represents cooling. The green arrows represent the anomalous residual meridional circulation. The circled numbers represent the sequence of the coupling mechanism. The T, U, and θ represent temperature, zonal wind, and latitude, respectively. The GWD, EPD, TP, SP, and MP represent GW drag, EP flux divergence, tropopause, stratopause, and mesopause, respectively.

As such, the breaking level for the eastward-propagating GWs is shifted downward and causes the anomalous westward GW forcing in the SH mesopause region. This further drives an anomalous residual circulation with downwelling at the SH high latitudes and induces anomalous warming in that region, as demonstrated by model simulations (Körnich and Becker 2010).

Our results derived from both WACCM simulation and satellite observations clearly show an upper-mesosphere cooling and a lower-thermosphere warming in the SH early summer polar region (Fig. 1) during warm ENSO events. In December, the summer stratosphere easterly zonal wind at the SH mid- and high latitudes is weak or recently reversed from winter westerly; stratospheric zonal wind anomalies during December ENSO events can significantly impact the stratospheric GW filtering and thus the GW forcing in the summer mesosphere. Later, in January, the stratosphere summer easterly jet is usually well established in the SH midlatitudes. With the strong midsummer jet in the SH, stratospheric zonal wind anomalies in the NH (e.g., during SSW events) will not impact the SH winds sufficiently to change the GW filtering and thus will not have much impact on GW forcing in the summer mesosphere. We also plot the WACCM and MLS temperature composite anomalies (warm minus cold events) during the ENSO events in January (not shown). The summer mesosphere cooling is not significant in WACCM but is clear in MLS. The difference in the period during the final warming and end of winter (December; examined here) and the period with a fully established summer circulation (most Januaries; examined in several previous studies) accounts for the difference in the role of the SH stratosphere in controlling the GW interannual variability. Our proposed coupling mechanism, in which the SH stratosphere is a necessary link, is valid in December (SH early summer), while the IHC proposed by Karlsson et al. (2009), in which the coupling occurs predominantly from the NH to SH mesosphere, is valid in January during an SSW event or strong PW activity.

5. Impact on PMC occurrence

Karlsson et al. (2011) suggest that the onset time of SH summer PMCs is mainly controlled by the breakdown time of the SH stratospheric polar vortex. Using nearly 30 years of the solar backscatter ultraviolet (SBUV) satellite observations and ECMWF Re-Analysis dataset, Benze et al. (2012) found that the 11-yr solar cycle could influence the SH PMC onset time. Our study further suggests that the temperature anomalies associated with ENSO in the SH early summer polar upper-mesosphere region may impact the SH PMC formation. As shown in Fig. 1, the significant cooling [$\sim -2\,\mathrm{K}\,(\mathrm{N3.4})^{-1}$] near 80–90 km during warm ENSO events could lead to earlier onset and larger PMC occurrence frequency in the SH summer mesopause region than those during cold ENSO events. On the other hand, the equatorial QBO could also modulate the SH stratosphere polar vortex with a maximum effect occurring in November (Baldwin and Dunkerton 1999) and thus could also affect the GW filtering and the consequent SH polar upper-mesosphere temperature. Water vapor is another important factor for the PMC formation. However, using *Aeronomy of Ice in the Mesosphere* (*AIM*) and *Aura*/MLS satellite data between 2007 and 2011, Rong et al. (2014) found that the correlation of albedo and H_2O (without time lag) is poor throughout the season in the NH, while temperature and albedo are clearly anticorrelated during the season start and end. Therefore, we will only study the correlation between temperature and PMCs during the PMC startup season in this paper.

Garfinkel and Hartmann (2008) and Calvo et al. (2009) suggest that the combination of QBO and ENSO could significantly influence the polar stratospheric temperature. The SABER and MLS data records are too short to stratify by both QBO and ENSO. However, we can investigate the stratospheric response using ECMWF reanalysis, although there are only a few observations in the SH lower stratosphere available to be implemented into the reanalysis. Figure 5 shows the composite difference of the ECMWF stratospheric zonal mean zonal wind between warm and cold ENSO (top) and between QBO easterly and westerly phase (bottom) in November (left) and December (right). The stratosphere zonal wind anomalies at the SH high latitudes are maximized when the QBO phase is defined with the equatorial zonal wind near ~25 hPa (Baldwin and Dunkerton 1999). The equatorial zonal winds at ~25 hPa are reconstructed from the two leading orthogonal principal components, which are derived with the radiosonde observed equatorial stratospheric zonal wind at seven pressure levels (Wallace et al. 1993). We note here that the composite difference of ECMWF stratosphere zonal wind at the SH high latitudes associated with ENSO in December ($\sim 6\,\mathrm{m\,s^{-1}}$) is clearly ~3 times stronger than that derived from WACCM shown in Fig. 4 ($\sim 2\,\mathrm{m\,s^{-1}}$ with N3.4 index of ~3.2), suggesting that the WACCM simulation likely underestimates the ENSO effect in the middle atmosphere. It is also illustrated in Fig. 1, where the satellite observations of temperature anomalies in the mesosphere are ~3–5 times stronger than the WACCM simulation. We also note the difference between ECMWF and WACCM at the NH high latitudes, with significant easterly anomaly in WACCM while none appears in ECMWF. The difference in the zonal wind anomalies leads to a difference temperature anomaly pattern, which has been reported previously by Garcia-Herrera et al. (2006).

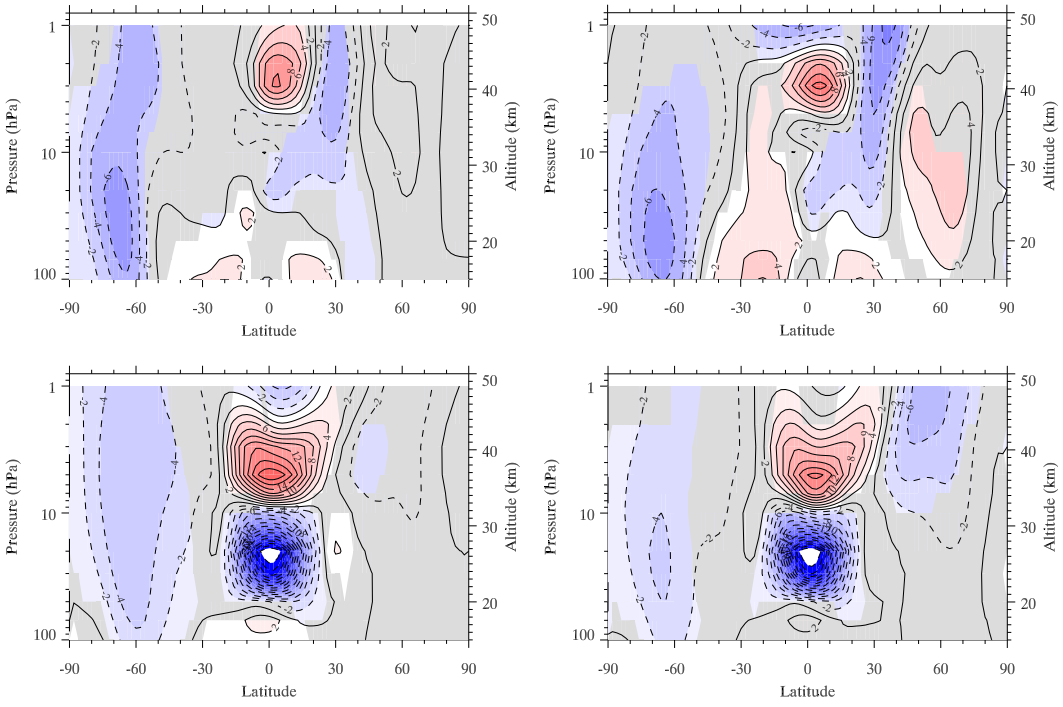

FIG. 5. Composite difference of the ECMWF stratospheric zonal mean zonal wind (top) between warm and cold ENSO and (bottom) between QBO easterly and westerly phase in (left) November and (right) December. The contour line interval is 2 m s^{-1}. The gray regions denote confidence levels below 95% (1.96σ).

In Fig. 5, we clearly see the anomalous stratospheric easterly zonal wind at the SH high latitudes during the QBO easterly phase in November, consistent with the pattern shown in Fig. 4 of Baldwin and Dunkerton (1999). However, the magnitude of composite difference shown in Fig. 5 is weaker than that found by Baldwin and Dunkerton (1999). In our results, the QBO zonal wind anomaly at the SH high latitudes is ~1–2 times weaker than that associated with ENSO in both November and December. Nevertheless, this suggests that both QBO and ENSO could modulate the SH stratospheric polar vortex and its breakdown time. The WACCM simulation also suggests that the SH polar upper-mesosphere temperature anomalies during ENSO events are stronger in November (not shown) than those in December, consistent with an anomalous SH high-latitude stratospheric zonal wind. Therefore, the constructive interference of ENSO and QBO in the SH high-latitude stratosphere could lead to even stronger anomalous easterly zonal wind and early breakdown of SH stratospheric polar vortex during warm ENSO in the easterly QBO phase and thus more eastward GW forcing in the SH upper mesosphere and colder temperature in the SH polar upper mesosphere than climatology. The simultaneous occurrence of a cold ENSO and westerly QBO would have the opposite effect—that is, late breakdown of SH stratospheric polar vortex and warmer temperature in the SH polar upper mesosphere. This further indicates that the PMC onset time could be much earlier during warm ENSO events in the easterly QBO phase than during cold ENSO events in the westerly QBO phase. The destructive interference of ENSO and QBO, however, could cancel their effects on the SH polar upper-mesosphere temperature and thus the PMC onset time.

Table 2 lists the ENSO year with corresponding N3.4 index, QBO phase defined with the equatorial zonal wind at ~25 hPa, SH polar upper-mesosphere T anomaly possibly associated with both ENSO and QBO, the PMC onset in terms of days from solstice (DFS) observed by the SBUV, and the breakdown time of SH stratospheric polar vortex between 1982 and 2012 as adapted and estimated from Fig. 2 in Benze et al. (2012). The PMC onset times (with the breakdown time of SH stratospheric polar vortex) all occur in late November with an average of ~−27 DFS (~−24 DFS) during warm ENSO events in the easterly QBO phase (total of four cases), corresponding to SH polar upper-mesosphere cooling. Although there are only two cases (1998/99 and 2010/11) that occurred during a cold ENSO event in the westerly QBO phase, the PMC onset times are at or after solstice with an average of ~3 DFS with the breakdown of SH stratospheric polar vortex at around solstice, corresponding to a SH polar

TABLE 2. The list of ENSO year with corresponding N3.4 index, QBO phase defined by zonal wind at ~25 hPa, the estimated T anomalies with ENSO and QBO combined, the PMC onset days from solstice, and breakdown time of SH stratosphere polar vortex adapted from Fig. 2 in Benze et al. (2012).

ENSO year	N3.4 index	QBO phase	Mesopause T anomaly	PMC onset (DFS)	Polar vortex breakdown
1982/83	2.14	W	Neutral	−5	−28
1984/85	−1.27	E	Neutral	−13	−19
1988/89	−1.93	E	Neutral	−28	−37
1991/92	1.69	E	Colder	−30	−33
1994/95	1.22	E	Colder	−29	−28
1997/98	2.33	W	Neutral	−25	−27
1998/99	−1.58	W	Warmer	6	2
2002/03	1.37	E	Colder	−21	−18
2006/07	1.09	W	Neutral	−16	−8
2007/08	−1.60	E	Neutral	0	3
2009/10	1.43	E	Colder	−28	−17
2010/11	−1.47	W	Warmer	0	−1

upper-mesosphere warming. The average of PMC onset times (with breakdown time of SH stratospheric polar vortex) in the other seven cases (destructive interference between ENSO and QBO) during either warm ENSO events in the westerly QBO phase or cold ENSO events in easterly QBO phase is ~−11 DFS (~−16 DFS). In addition, we also find that the average PMC onset time (breakdown time of SH stratospheric polar vortex) is ~−21 DFS (~−23 DFS) during warm ENSO events and ~−5 DFS (~−10 DFS) during cold events regardless of QBO phase. The onset (breakdown time of SH stratospheric polar vortex) is ~−21 DFS (~−21 DFS) during easterly QBO phase and ~−8 DFS (~−12 DFS) during westerly phase regardless of ENSO events. These results indicate that both ENSO and QBO could dramatically impact the SH PMC onset times by modulating the SH high-latitude stratosphere zonal wind and the breakdown time of stratospheric polar vortex. However, longer observational PMC datasets, concurrent with polar mesosphere temperature and water vapor, are necessary to quantitatively evaluate the ENSO and QBO influences on PMCs, and this is beyond the scope of this paper.

6. Summary

Using satellite observed temperature profiles, we reveal significant temperature anomalies in the SH summer polar mesopause region during ENSO events in December. The observed temperature anomalies agree with those simulated by the WACCM, although the observed magnitude is ~3–5 times stronger than that simulated. The WACCM simulations show an equatorial stratospheric cooling during warm ENSO events in December that is consistent with enhanced equatorial upwelling due to the enhanced PW propagation and dissipation in the NH stratosphere. This equatorial cooling increases the SH stratosphere meridional temperature gradient, leading to stronger stratospheric easterly zonal winds at the SH mid- and high latitudes. Filtering by the SH stratospheric zonal wind causes anomalous SH mesospheric eastward GW forcing and eventually leads to an enhanced residual meridional circulation and upper-mesosphere cooling in the SH summer polar region. The subsequent anomalous GW filtering by the upper-mesosphere zonal wind further induces anomalous GW forcing in the lower thermosphere of the SH high latitudes, leading to an anomalous residual meridional circulation that is opposite to its upper-mesosphere counterparts.

ENSO and the QBO could significantly modulate the SH stratosphere polar vortex. The constructive interference of ENSO and QBO could lead to anomalous easterly or westerly stratospheric zonal winds in November and December at the SH high latitudes during warm ENSO events in the easterly QBO phase (defined with the equatorial wind at ~25 hPa) or during cold ENSO events in the westerly QBO phase. Either of these combinations would affect the extent of eastward GW forcing and the temperature and, hence, affect the onset time of SH PMCs relative to the climatological average. The destructive interference of ENSO and QBO, during either warm ENSO events in the westerly QBO phase or cold ENSO events in the easterly QBO phase, could cancel their effects on the SH polar upper-mesosphere temperature and thus the PMC onset time. Our results clearly indicate that ENSO and the QBO modulate the onset time of SH PMCs.

Acknowledgments. TL would like to thank Han-Li Liu and Chengyun Yang for helpful discussion. TL and XD are

supported by the National Natural Science Foundation of China Grants 41225017 and 41421063 and the National Basic Research Program of China Grant 2012CB825605. TL's visit to ERAU is partially supported by the NSF Grants AGS-1115249 and AGS-1110199. NC acknowledges partial support from the Spanish Ministry of Economy and Competitiveness through the PALEOSTRAT project (Paleomodelization desde una perspectiva estratoferica; Ref. CGL2015-69699-R) and the European Project 603557-STRATOCLIM under program FP7-ENV.2013.6.1-2. JY is supported by the NASA *AIM* and *TIMED* satellite missions. JMR is supported under NASA SABER Grant NNX15AD22G. MGM is supported by the NASA *TIMED* satellite project. AZL is supported by National Science Foundation Grants AGS-1115249 and AGS-1110199. The WACCM 3.5 results were obtained from the Atmospheric Chemistry Division at the National Center for Atmospheric Research. The radiosonde dataset is downloaded from http://www.geo.fu-berlin.de/en/met/ag/strat/produkte/qbo/index.html. We want to thank Bodil Karlsson and two other anonymous reviewers for their constructive comments on this paper.

REFERENCES

Andrews, D., and M. McIntyre, 1976: Planetary waves in horizontal and vertical shear: The generalized Eliassen–Palm relation and mean zonal acceleration. *J. Atmos. Sci.*, **33**, 2031–2048, doi:10.1175/1520-0469(1976)033<2031:PWIHAV>2.0.CO;2.

Baldwin, M. P., and T. J. Dunkerton, 1999: Propagation of the Arctic Oscillation from the stratosphere to the troposphere. *J. Geophys. Res.*, **104**, 30 937–30 946, doi:10.1029/1999JD900445.

Becker, E., A. Müllemann, F. J. Lübken, H. Körnich, P. Hoffmann, and M. Rapp, 2004: High Rossby-wave activity in austral winter 2002: Modulation of the general circulation of the MLT during the MaCWAVE/MIDAS northern summer program. *Geophys. Res. Lett.*, **31**, L24S03, doi:10.1029/2004GL019615.

Benze, S., C. E. Randall, B. Karlsson, V. L. Harvey, M. T. DeLand, G. E. Thomas, and E. P. Shettle, 2012: On the onset of polar mesospheric cloud seasons as observed by SBUV. *J. Geophys. Res.*, **117**, D07104, doi:10.1029/2011JD017350.

Calvo, N., M. A. Giorgetta, R. Garcia-Herrera, and E. Manzini, 2009: Non-linearity of the combined warm ENSO and QBO effects on the Northern Hemisphere polar vortex in MAECHAM5 simulations. *J. Geophys. Res.*, **114**, D13109, doi:10.1029/2008JD011445.

——, R. Garcia, W. Randel, and D. Marsh, 2010: Dynamical mechanism for the increase in tropical upwelling in the lowermost tropical stratosphere during warm ENSO events. *J. Atmos. Sci.*, **67**, 2331–2340, doi:10.1175/2010JAS3433.1.

Dee, D. P., and Coauthors, 2011: The ERA-Interim reanalysis: Configuration and performance of the data assimilation system. *Quart. J. Roy. Meteor. Soc.*, **137**, 553–597, doi:10.1002/qj.828.

Espy, P. J., S. O. Fernández, P. Forkman, D. Murtagh, and J. Stegman, 2011: The role of the QBO in the inter-hemispheric coupling of summer mesospheric temperatures. *Atmos. Chem. Phys.*, **11**, 495–502, doi:10.5194/acp-11-495-2011.

Garcia-Herrera, R., N. Calvo, R. Garcia, and M. Giorgetta, 2006: Propagation of ENSO temperature signals into the middle atmosphere: A comparison of two general circulation models and ERA-40 reanalysis data. *J. Geophys. Res.*, **111**, D06101, doi:10.1029/2005JD006061.

Garfinkel, C. I., and D. L. Hartmann, 2008: Different ENSO teleconnections and their effects on the stratospheric polar vortex. *J. Geophys. Res.*, **113**, D18114, doi:10.1029/2008JD009920.

Gumbel, J., and B. Karlsson, 2011: Intra- and inter-hemispheric coupling effects on the polar summer mesosphere. *Geophys. Res. Lett.*, **38**, L14804, doi:10.1029/2011GL047968.

Hardiman, S. C., N. Butchart, P. H. Haynes, and S. H. E. Hare, 2007: A note on forced versus internal variability of the stratosphere. *Geophys. Res. Lett.*, **34**, L12803, doi:10.1029/2007GL029726.

Hervig, M. E., M. H. Stevens, L. L. Gordley, L. E. Deaver, J. M. Russell III, and S. M. Bailey, 2009: Relationships between polar mesospheric clouds, temperature, and water vapor from Solar Occultation for Ice Experiment (SOFIE) observations. *J. Geophys. Res.*, **114**, D20203, doi:10.1029/2009JD012302.

Karlsson, B., C. McLandress, and T. G. Shepherd, 2009: Inter-hemispheric mesospheric coupling in a comprehensive middle atmosphere model. *J. Atmos. Sol.-Terr. Phys.*, **71**, 518–530, doi:10.1016/j.jastp.2008.08.006.

——, and Coauthors, 2011: On the seasonal onset of polar mesospheric clouds and the breakdown of the stratospheric polar vortex in the Southern Hemisphere. *J. Geophys. Res.*, **116**, D18107, doi:10.1029/2011JD015989.

Körnich, H., and E. Becker, 2010: A simple model for the interhemispheric coupling of the middle atmosphere circulation. *Adv. Space Res.*, **45**, 661–668, doi:10.1016/j.asr.2009.11.001.

Li, T., T. Leblanc, and I. S. McDermid, 2008: Interannual variations of middle atmospheric temperature as measured by the JPL lidar at Mauna Loa Observatory, Hawaii (19.5°N, 155.6°W). *J. Geophys. Res.*, **113**, D14109, doi:10.1029/2007JD009764.

——, N. Calvo, J. Yue, X. Dou, J. M. Russell, M. G. Mlynczak, C.-Y. She, and X. Xue, 2013: Influence of El Niño–Southern Oscillation in the mesosphere. *Geophys. Res. Lett.*, **40**, 3292–3296, doi:10.1002/grl.50598.

Manzini, E., M. A. Giorgetta, M. Esch, L. Kornblueh, and E. Roeckner, 2006: The influence of sea surface temperatures on the northern winter stratosphere: Ensemble simulations with the MAECHAM5 model. *J. Climate*, **19**, 3863–3881, doi:10.1175/JCLI3826.1.

Murphy, D. J., S. P. Alexander, and R. A. Vincent, 2012: Interhemispheric dynamical coupling to the southern mesosphere and lower thermosphere. *J. Geophys. Res.*, **117**, D08114, doi:10.1029/2011JD016865.

Pedatella, N. M., and H.-L. Liu, 2013: Influence of the El Niño Southern Oscillation on the middle and upper atmosphere. *J. Geophys. Res. Space Phys.*, **118**, 2744–2755, doi:10.1002/jgra.50286.

Randel, W. J., R. R. Garcia, N. Calvo, and D. Marsh, 2009: ENSO influence on zonal mean temperature and ozone in the tropical lower stratosphere. *Geophys. Res. Lett.*, **36**, L15822, doi:10.1029/2009GL039343.

Rong, P. P., J. M. Russell III, C. E. Randall, S. M. Bailey, and A. Lambert, 2014: Northern PMC brightness zonal variability and its correlation with temperature and water vapor. *J. Geophys. Res. Atmos.*, **119**, 2390–2408, doi:10.1002/2013JD020513.

Russell, J. M., M. G. Mlynczak, L. L. Gordley, J. Tansock, and R. Esplin, 1999: Overview of the SABER experiment and preliminary calibration results. *Optical Spectroscopic Techniques and Instrumentation for Atmospheric and Space Research III*,

A. M. Larar, Ed., International Society for Optical Engineering (SPIE Proceedings, Vol. 3756), 277–288, doi:10.1117/12.366382.

Sassi, F., D. Kinnison, B. Boville, R. Garcia, and R. Roble, 2004: Effect of El Niño–Southern Oscillation on the dynamical, thermal, and chemical structure of the middle atmosphere. *J. Geophys. Res.*, **109**, D17108, doi:10.1029/2003JD004434.

Schwartz, M. J., and Coauthors, 2008: Validation of the Aura Microwave Limb Sounder temperature and geopotential height measurements. *J. Geophys. Res.*, **113**, D15S11, doi:10.1029/2007JD008783.

Siskind, D. E., M. H. Stevens, M. Hervig, F. Sassi, K. Hoppel, C. R. Englert, and A. J. Kochenash, 2011: Consequences of recent Southern Hemisphere winter variability on polar mesospheric clouds. *J. Atmos. Sol.-Terr. Phys.*, **73**, 2013–2021, doi:10.1016/j.jastp.2011.06.014.

Wallace, J. M., R. L. Panetta, and J. Estberg, 1993: Representation of the equatorial quasi-biennial oscillation in EOF phase space. *J. Atmos. Sci.*, **50**, 1751–1762, doi:10.1175/1520-0469(1993)050<1751:ROTESQ>2.0.CO;2.

Yulaeva, E., and J. Wallace, 1994: The signature of ENSO in global temperature and precipitation fields derived from the Microwave Sounding Unit. *J. Climate*, **7**, 1719–1736, doi:10.1175/1520-0442(1994)007<1719:TSOEIG>2.0.CO;2.